communications chemistry

A Nature Portfolio journal

Article

https://doi.org/10.1038/s42004-025-01591-2

Mechanically interlocked nanotubes as recyclable catalysts for Knoevenagel condensation

Mariano Vera-Hidalgo[1], Matías Blanco[2] ✉, Teresa Naranjo[1], Cristina Navío[1], Luisa Ruiz-González[3], Alejandro López-Moreno[1] & Emilio M. Pérez[1] ✉

Single-walled carbon nanotubes (SWNTs) are a very attractive platform to build heterogeneous catalysts, benefiting from their intrinsic high surface area and their insolubility. Here, we show that SWNTs encapsulated within organic macrocycles to form mechanically interlocked rotaxane-type species (MINTs), are a good building block to graft basic nitrogenous moieties for the catalysis of the Knoevenagel condensation. The installation of the catalytically active groups is carried out after formation of the MINTs, following a modular approach. Through this chemical modification strategy, we obtain very active MINT catalysts (TOF in the range of 900–9000 h^{-1}). The interlocked catalysts can be recycled for at least five times by simple filtration and washing, without any appreciable loss of activity. In comparison, supramolecular controls lacking the mechanical link between the active moiety and the SWNT cannot be recycled. From a general point of view, these results prove that formation of MINTs is an interesting strategy to link catalytic molecular moieties to SWNTs, enabling their use as heterogeneous catalysts and therefore facilitating the purification of the products and the recycling of the catalyst.

The development of efficient metal-free catalysts has garnered significant attention in recent years due to their potential to replace scarce and toxic metal-based catalysts in various chemical reactions. A wide range of materials[1], including zeolites[2,3], silica[4], clays[5], polymers[6,7], and (nano)carbon materials[8–12], have been explored as metal-free catalysts. Among these, single-walled carbon nanotubes (SWNTs) offer promising potential due to their extreme surface to volume ratio (all atoms are surface atoms), their excellent electrical conductivity and their chemical stability. On the downside, the tendency of SWNTs to aggregate forming bundles typically reduces the available surface area significantly and their synthesis and purification remains costly, which currently limits scalability.

Using SWNTs as metal-free catalysts typically requires some chemical modification to improve their dispersibility or to introduce active functional groups to contribute to the catalytic phenomena[13]. Our group has pioneered the use of mechanical bonds to functionalise SWNTs, forming mechanically interlocked derivatives of SWNTs (MINTs)[14,15]. MINTs are rotaxane-type species in which SWNTs are encapsulated by organic macrocycles[16–19]. By carefully designing the macrocycles, we have demonstrated improved catalytic performance and stability compared to pristine or supramolecularly modified SWNTs. For example, the catalytic activity of MINTs in the reduction of nitroarenes with hydrazine was investigated[20]. Three different MINTs with electron donor, acceptor, or electronically neutral macrocycles were compared, establishing a relationship between the expected electronic density at the SWNT surface and the catalytic activity. Later, we demonstrated the promising properties of MINTs in the Oxygen Reduction Reaction (ORR) with different macrocycles using anthraquinone as recognition motifs[21] or by introducing *N*-rich macrocycles[22].

Our strategy to synthesize MINTs involves the ring-closing metathesis of U-shaped macrocyclic precursors around the SWNTs. The U-shaped molecules feature two copies of a recognition motif for SWNTs featuring long alkene-terminated alkyl chains, and linked by a xylylene spacer. This design can be customised by modifying both the recognition motif and the aromatic spacer, allowing for the introduction of functional groups tailored to specific applications. For example, incorporating an amine group and its subsequent derivatisation can enhance the Lewis and Brönsted basicity of the MINT system, making it a potential catalyst for reactions such as Knoevenagel, Michael, and Henry additions[23]. Several examples of basic catalysts are reported by anchoring primary to quaternary amines on the

[1]IMDEA Nanociencia, Campus de Cantoblanco, Calle Faraday 9, Madrid, Spain. [2]Organic Chemistry Department, Universidad Autónoma de Madrid, Módulo 1, Madrid, 28049 Spain. Institute for Advanced Research in Chemical Sciences (IAdChem), Universidad Autónoma de Madrid, Madrid, Spain. [3]Departamento de Química Inorgánica and Centro Nacional de Microscopía Electrónica, Universidad Complutense de Madrid, Madrid, Spain. ✉e-mail: matias.blanco@uam.es; emilio.perez@imdea.org

surface of very different variety of materials employing covalent and supramolecular approximations[24–27]. The Knoevenagel condensation was chosen as model system, as its mechanism is very well understood (see the Supporting Information). Here, we describe the design, synthesis and catalyitic performance of three MINT systems as basic catalyst for Knoevenagel condensations.

Results and Discussion

Synthesis and characterisation

We synthesised MINTs with a primary amine group attached to the spacer (MINT-NH_3Cl), and then either alkylated them using iodoethane (MINT-NEt_2) or formed imines with picolinaldehyde (MINT-NPy) to further increase its basicity. These modified MINTs were evaluated as catalysts in the Knoevenagel condensation of aromatic aldehydes and malononitrile, demonstrating enhanced activity compared to controls. Moreover, we investigated the scope of the catalysts using various aldehydes with different characteristics.

In order to synthetize a nitrogen-functionalised MINT, we modified the spacer of a pyrene-based U-shaped receptor previously reported by us (Fig. 1). Briefly, the protection of the amino moiety of the 5-aminoisophtalic acid with a *tert*-butoxycarbonyl protecting group (Boc), followed by the reduction of the acids to the corresponding alcohols and substitution with bromides yielded a connecting molecule[28] which can be etherified with two derivatised C11-alkenyl-terminated pyrene units, as reported previously[15].

For the MINT synthesis (Fig. 2), we used (6,5)-enriched single-walled nanotubes (0.7–0.9 nm in diameter, length ≥ 700 nm, 95% purity, Sigma-Aldrich), purified via acid wash, in all experiments. We followed the strategy we reported previously[29], which consists of a ring-closing metathesis clipping reaction in which the SWNTs serve as a template for the macrocyclation of the U-shaped molecule around the nanotubes, to yield MINT-NHBoc. MINT-NHBoc was chosen as the building block from which the rest of the derivatives are synthesized to allow for direct comparison of the activity of the same batch of material with and without the basic nitrogenated moieties. Very briefly, we treated a suspension of SWNTs in tetrachloroethane (10 mg/10 mL) with the bisalkene precursor of mac-NHBoc (10 mg, 0.01 mmol) and Grubbs' 2nd generation catalyst (8.5 mg, 0.01 mmol), and the mixture was stirred at room temperature for 72 h. After this time, the suspension was filtered through a polytetrafluoroethylene (PTFE) membrane (0.2 µm pore size) and the product was purified by resuspending it in dichloromethane (DCM) with ultrasonication, filtering and washing profusely with DCM to wash away excess bisalkene precursor, non-threaded macrocycles, catalyst and all soluble impurities. This washing procedure was repeated three times. In order to synthesize the free amine MINT material (Fig. 2), MINT-NHBoc was deprotected by treatment with 4 M HCl overnight to yield a free amino group (MINT-NH_3Cl in Fig. 2)[30]. We further modify the ammonium group with different nitrogen-containing moieties (Fig. 2). In particular, we added 2-picolinealdehyde in acidic conditions to provide a di-nitrogen basic site (MINT-NPy, Fig. 2)[31]. Alternatively, we alkylated the aniline with ethyl iodide under basic conditions to improve the basicity of the aniline moiety (MINT-NEt_2)[32]. To confirm the viability of these reaction conditions, we separately prepared mac-NHBoc, deprotected it to mac-NH_3Cl, and derivatized it to mac-NPy and mac-NEt_2. The synthetic details and the characterisation data are shown on the SI.

All MINT materials were fully characterised using thermogravimetric analysis (TGA), Raman spectroscopy, UV-vis-NIR, photoluminescence excitation-emission maps (PLE), X-Ray photoelectron spectroscopy (XPS), high-resolution transmission electron (HR-TEM) and atomic force microscopies (AFM). The TGA results are shown in Fig. 3a, together with a reference sample of (6,5)-SWNTs. The TGA of MINT-NHBoc shows a mass loss of 3% between 150 °C and 250 °C, corresponding to the Boc group, and a 24% loss between 300 °C and 450 °C, related to the macrocycle. For the MINT-NH_3Cl sample, a 23% loss is observed between 300 °C and 450 °C, with a minor 5% loss around 300 °C, which is attributed to the -NH_3Cl group[33]. The derivatization of MINT-NH_3Cl to produce MINT-NEt_2 and MINT-NPy is confirmed by the TGA profiles of these samples. In the case of MINT-NEt_2, a mass loss of approximately 27% is observed, corresponding to the organic functionalization. This 4% increase aligns well with the introduction of the two ethyl groups. Meanwhile, the TGA of MINT-Npy shows a 28% mass loss, representing a 5% increase in organic content compared to MINT-NH_3Cl, which is again consistent with the incorporation of the pyridine ring into the macrocycle.

On the other hand, Raman spectra under $\lambda_{exc} = 532$ nm (Fig. 3b and Figure S13) showed a small increase in the I_D/I_G ratio between pristine SWNTs ($I_D/I_G = 0.03 \pm 0.01$) and MINT-NHBoc samples $I_D/I_G = 0.12 \pm 0.05$. This increase is noticeable, but corresponds to a very low density of defects (ca. 20 defects / μm^{-1})[34], that does not compare to the degree of functionalization observed in TGA (one macrocycle every 214 C atoms or every 2 nm, as calculated from the weight loss in the TGA data). We therefore assign this increase to the introduction of defects during the washing procedures, that involve ultrasonication. This is confirmed by the I_D/I_G ratio in the successive steps of our synthesis, where we obtain I_D/I_G values of 0.06 ± 0.02, 0.06 ± 0.02 and 0.07 ± 0.02 for MINT-NH_3Cl, MINT-NPy and MINT-NEt_2 respectively. Since these samples are obtained from the MINT-NHBoc, these values futher

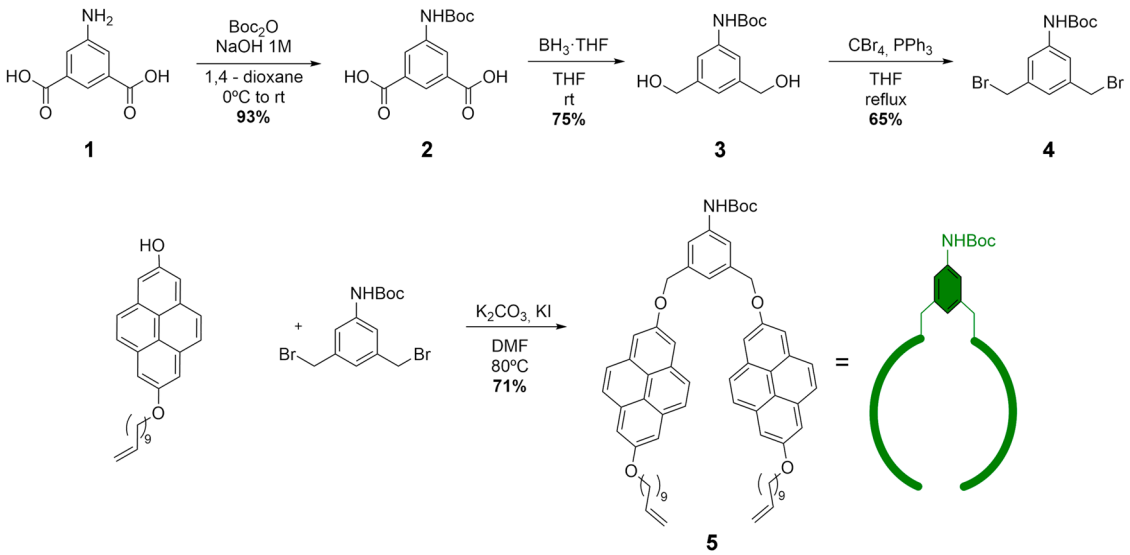

Fig. 1 | Synthesis of U-shapes. Synthetic route for the synthesis of N-based U-shapes.

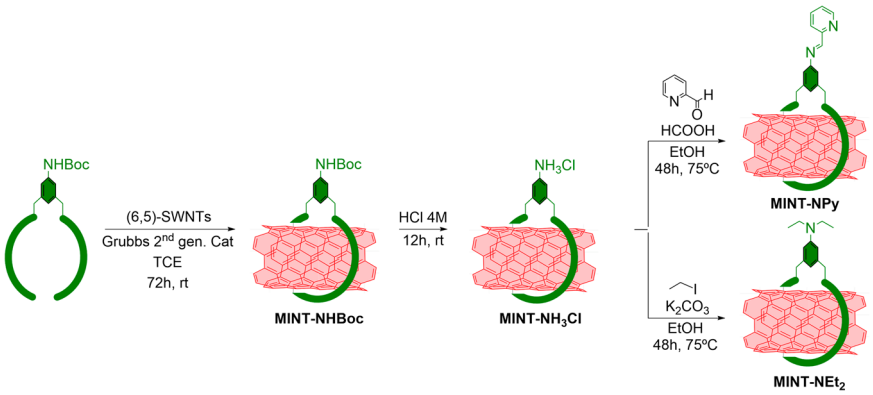

Fig. 2 | Structure and synthesis of MINTs. Synthesis of MINT-NHBoc through ring closing metathesis reaction and the further deprotection or reaction to obtain MINT-NH_3Cl, MINT-NPy and MINT-NEt_2.

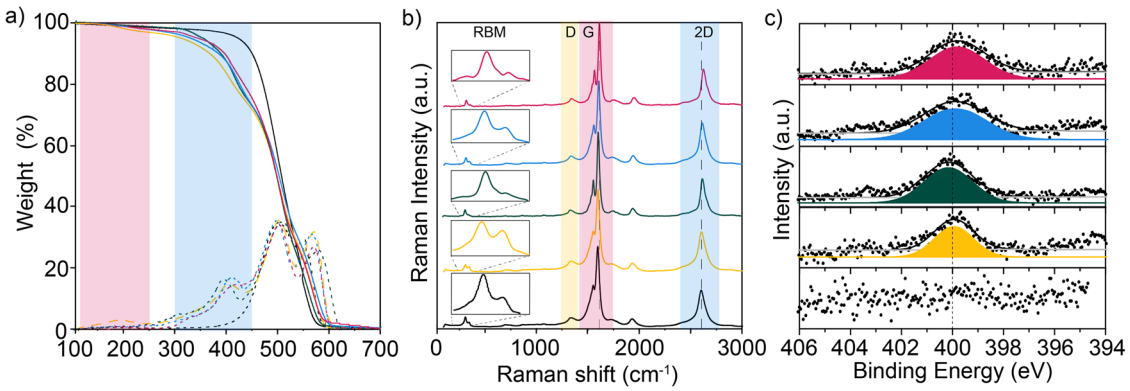

Fig. 3 | Characterization of MINTs. a TGA plots of different MINTs and pristine (6,5)-SWNTs. **b** Raman spectra of different MINTs and pristine (6,5)-SWNTs; and **c** XPS N 1s core level region of samples. (6,5)-SWNT (black), MINT-NHBoc (yellow), MINT-NH_3Cl (green) MINT-NPy (blue), MINT-NEt_2 (red).

confirm that there is no significant covalent reaction during formation of the MINTs and corroborate that these subsequent chemical procedures only modified the organic macrocycles and not the SWNTs. We don't observe notworthy changes in either the radial breathing modes (RBM) or the G band during the chemical manipulation.

The UV-vis-NIR absorption spectra of our materials in D_2O/SDS (1 wt %) at room temperature showed the typical absorption features of SWNTs corresponding to S_{22} and S_{11} transitions (See SI). The spectra of pristine SWNTs is dominated by two pairs of signals corresponding to (6,5)-SWNTs (575–975 nm) and (7,5)-SWNTs (660–1020 nm). After functionalization with a macrocycle containing an NHBoc group, a change in the ratio of these bands is observed, with an increase in the relative intensity of the (6,5)-SWNTs compared to the (7,5)-SWNTs[35]. Despite the poorer dispersion quality in the case of MINT-NH_3Cl, a similar trend to that of MINT-NHBoc is observed. Following derivatization to obtain MINT-NEt_2, the presence of both pairs of bands is similarly observed without any noticeable shift. Finally, MINT-NPy exhibits broadening of the bands around 1000 nm, which is associated with poorer dispersion, making it difficult to distinguish between the bands corresponding to different chiralities. However, the S_{22} bands indicate that both chiralities are present in comparable amounts in the sample. As a general trend, no significant shifts in the absorption bands are observed, only changes in the relative intensity of these bands. These results are in line with the lack of significant shifts in the G bands of the Raman spectra.

PLE maps of SWNTs and the MINTs under study were also recorded (see SI), and compared by normalisation to the optical density of the samples. We excited the samples between 500 and 800 nm and detected the emission from 820 to 1590 nm and observed mainly the fluorescence of (6,5)-SWNTs in both samples. A quenching in the intensity of the signal was detected for all the MINTs with respect to the SWNTs, as previously reported for pyrene-based MINTs[29].

In order to shed light on the chemical nature of the *N*-containing group in every step of the synthesis, we performed XPS analysis. The *N*-containing MINT spectra perfectly overlaps the XPS C 1s and O 1s core level regions spectra of the pristine (6,5)-SWNT (see SI), which we interpret as further proof that the formation of MINTs, and the ensuing chemical steps, did not affect the structure of the nanotube, in agreement with the Raman data. The N 1s core level regions of the SWNTs and all MINT samples are shown in Fig. 3c. We do not observe any N 1s appreciable signal in the spectrum of the pristine material (black). In contrast, we notice a very clear peak in the N 1s region of the MINT-NHBoc spectrum. Quantitatively, we find around 1.6 at. % in N, which is consistent with the degree of functionalization found in TGA. This peak is centered in 399.9 eV and can be fitted satisfactorily with a single component, agreeing with the presence of carbamate-like species[36]. From MINT-NHBoc, shifts in the binding energy and differences in the full width at half maxima (FWHM) in the modified samples (MINT-NH_3Cl, MINT-NPy and MINT-NEt_2) were observed. After the fitting with Gaussian functions (see SI for details), we can confirm the presence of surface primary ammonium groups in MINT-NH_3Cl at 400.2 eV and tertiary amines in MINT-NEt_2 at 399.8 eV[37], both with satisfactorily fitted with a single component. However, we could not clearly assign the imine and pyridine components in MINT-NPy individually. Instead, a broad peak centred at 399.9 eV was fitted despite the experimental asymmetry measured. The position of this peak corresponds well to the expected imine and pyridine units[38].

Microscopic analysis under AFM and TEM of the MINTs shows results consistent with our previous observations for MINTs. On the topographic analysis performed on a drop-casted suspension of the samples over freshly exfoliated mica, we observed for MINT-NHBoc (Fig. 4a) a single SWNT with a height of approximately 1 nm, on which several bumps of approximately 1.6–1.7 nm are observed.

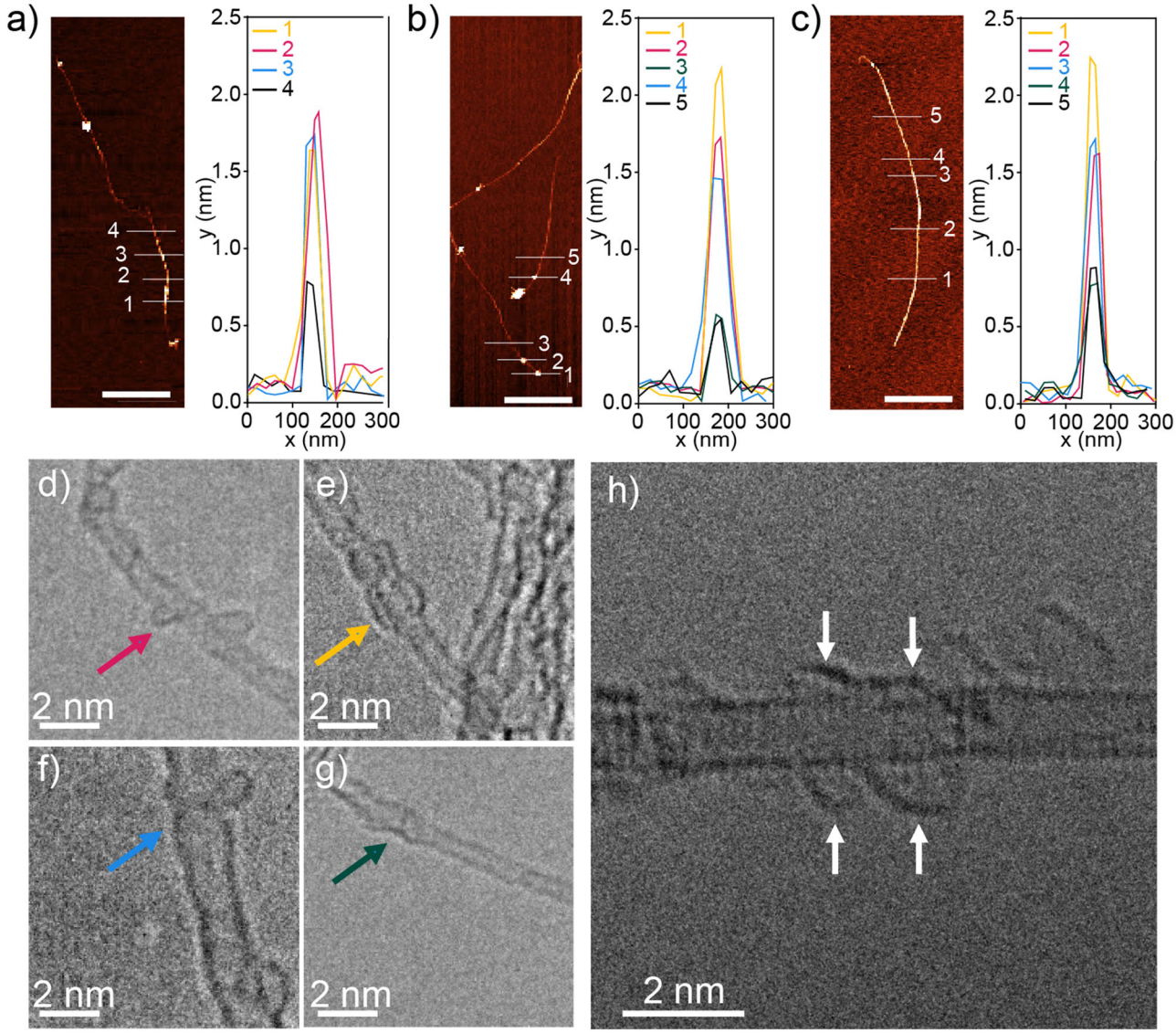

Fig. 4 | Microscopic analysis of MINTs. AFM topographic image of a suspension in TCE of (**a**) MINT-NHBoc; **b** MINT-NPy; **c** MINT-NEt_2. Height profiles along the lines marked in the topographic image. Scale bars are 500 nm. HRTEM micrographs of **d** MINT-NHBoc (red); (**e**) MINT-NH_3Cl (yellow); **f** MINT-NPy (blue); and **g** MINT-NEt_2 (purple). Scale bars are 2 nm. **h** ac-HRTEM micrograph of MINT-NPy. Scale bar is 2 nm.

After derivatisation to obtain MINT-NPy and MINT-NEt_2, similar protrusions were observed. For MINT-NPy (Fig. 4b) we observed individual SWNTs (height ca. 0.7 nm as measured in the clean areas), that presented several individualised protrusions of 1.5–2 nm, matching the macrocycles size. For MINT-NEt_2 a SWNT (with a height of 0.7–0.8 nm measured in clear zones) is nearly completely covered with a uniform coating of around 1.5–2 nm (Fig. 4c). TEM analysis allowed the direct observation of the surrounding organic macrocycles (or their respective decomposition products due to beam irradiation in the microscope chamber) along the nanotubes[39]. In the MINT-NHBoc sample (Fig. 4d) we detected SWNT arrays showed densely covered walls with organic moieties, in agreement with the functionalisation degree determined by TGA. More interestingly, circular objects with a diameter c.a. 1.9–2.1 nm were observed in isolated tubes. Both fully covered SWNT arrays and some individual macrocycles around SWNTs were observed for the derivatised samples MINT-NH_3Cl (yellow arrow), MINT-NPy (blue arrow) and MINT-NEt_2 (purple arrow). In the MINT-NPy sample we found two circular objects that perfectly matched with the expected macrocycle size (2 nm).

Catalytic activity

The *N*-functionalised MINTs featuring both pyridine and amine moieties were tested as catalysts in the Knoevenagel condensation of different aliphatic and aromatic aldehydes employing malononitrile as nucleophile[40]. Very briefly, 1 mmol of aldehyde and 1 mmol of malononitrile were mixed in 3 mL of ethanol with 5 mg of catalyst, and the reaction was stirred magnetically at the desired temperature until completion was detected. To set up these conditions, we first optimised reaction solvent (see the Supporting Information). Complete conversions were only obtained in ethanol. Poorer results were observed for water and acetonitrile, while toluene and THF, typical solvents for this condensation[40–43], did not show activity. We first tested our materials at room temperature. The reaction can easily be followed by ^{1}H NMR spectroscopy tracking the disappearance of the aldehyde proton at $\delta \sim 10$ ppm and the appearance of the benzylidene proton at $\delta \sim 8$ ppm (see experimental section and SI for further details). In order to understand the behavior of our catalysts, the reaction of benzaldehyde with malononitrile was selected as a model, with a 0.14% mol of catalyst as estimated from the average number of active sites deduced from TGA data (Fig. 5) MINT-NPy achieved complete conversion in 21 h, and MINT-NEt_2 required 40 h to complete the reaction, thus reproducing the

catalytic performance at high temperature. However, both SWNT and the non-catalysed reaction required 6 days (144 h) to reach the same level of conversion, demonstrating once again the importance of having a basic center in the functionalising moiety for obtaining enhanced results. MINT-NH_3Cl and MINT-NHBoc were also tested in the Knoevenagel condensation for comparative purposes. Interestingly, neither of them were able to catalyse the transformation during the first 5 h of reaction. We only detected the presence of the nucleophilic addition in the NMR spectra, which was saturated throughout the whole monitoring for both catalysts.

We also tested the reaction under refluxing temperature, reaching the best reaction times (Fig. 5). The reaction catalyzed by MINT-NPy reached completion in 1 h, while MINT-NEt_2 required 3 h to achieve the same conversion level, both with a sharp approximation to the typical Knoevenagel first order kinetics. In contrast, the reaction catalysed by pristine SWNT was completed in 24 h, obtaining very similar kinetic performances than the non-catalysed control reaction. Therefore, the presence of the basic nitrogen units in the macrocycle are crucial to obtain good catalytic performance, and the catalytic activity is not only due to the presence of the SWNTs. Notably, MINT-NH_3Cl was unable to catalyze the reaction, whereas the use of MINT-NHBoc resulted in a 68% conversion after 210 min, which decreased to 50% after 330 min and 24 h. To assess whether the presence of a free amine could be responsible for the observed catalytic activity, we performed thermal deprotection by heating the MINT-NHBoc for 2.5 h at 220 °C. The resulting MINT-NH_2 significantly enhanced the catalytic performance compared to both MINT-NH_3Cl and MINT-NHBoc, achieving a 72% conversion within just one hour. However, it failed to reach full conversion, exhibiting signs of catalyst poisoning and ultimately performing worse than the uncatalyzed reaction or reactions carried out with pristine SWNTs. Our interpretation is that the presence of protonated nitrogen in the NH_2-based MINT does not provide sufficient basicity, thereby inhibiting the progress of the reaction. When non-protonated NH_2 groups are present, the reaction proceeds until the catalyst is poisoned by the aldehyde, preventing complete conversion. On the other hand, the reaction catalyzed by the carbamate-functionalized MINT-NHBoc follows a similar course to that of the free amine, achieving maximum conversion after 210 min. In order to rule out the possibility of the imine being hydrolyzed (releasing free amine which might catalyze the reaction), we analyzed the imine under the reaction conditions. TGA did not reveal any clear evidence of weight loss attributable to such hydrolysis. (see Figure S18 in the Supporting Information)

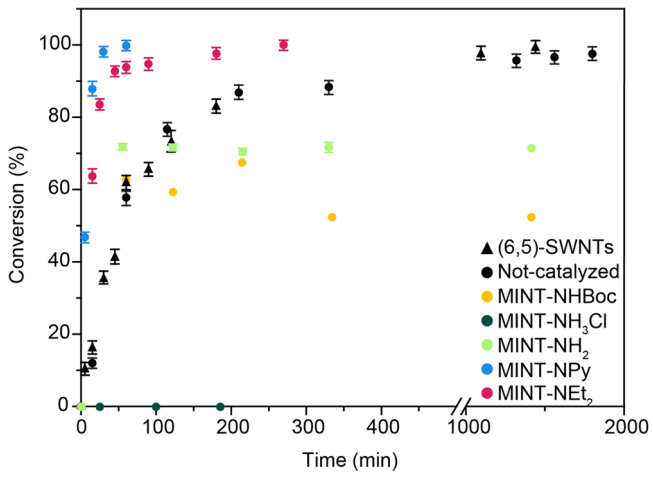

Fig. 5 | Catalytic activity of MINTs. Conversion *vs* time plots for the optimised benzaldehyde Knoevenagel condensation catalysed by (6,5)-SWNT (black triangle), MINT-NHBoc (yellow dot), MINT-NH_3Cl (dark green dot) MINT-NH_2 (light green dot), MINT-NPy (blue dot), MINT-NEt_2 (red dot) and a not-catalysed reaction (black circle). Error bars represent standard deviation of the data obtained in three independent experiments.

Comparing the two catalytically active MINT samples, MINT-NPy was twice as active as MINT-NEt_2 as a function of the reaction rates and the turnover frequency (TOF). Although the latter presents a tertiary amine, the presence of the two nitrogen atoms in the MINT-NPy, one of them belonging to a pyridine unit, provides more basic centers to the catalytic media, enhancing the reaction rate.

We also decided to study the cyclability of our heterogeneous catalyst in this model Knoevenagel reaction between benzaldehyde and malononitrile. Thus, after the completion of the reaction, catalysts were recovered by filtration through PTFE membranes, washed profusely three times with DCM to eliminate all the reagents involved in the condensation, and finally dried in vacuum. The recovered solids were subjected to five consecutive catalytic cycles at reflux conditions. Following this procedure, we found that both MINT-NPy and MINT-NEt_2 showed no loss of activity on the five consecutive cycles studied, achieving equivalent conversion levels in identical times (Table 1).

Supramolecular control examples, obtained by directly mixing the nanotube and the corresponding macrocycle in the same proportion determined by TGA in the MINTs, were also recycled employing the same recovery strategy. After following the same washing procedure described for the MINT samples, the remaining material was submitted to a new catalytic cycle. Very interestingly, the recovered catalyst achieved the same catalytic performance than the pristine (6,5)-SWNT in levels of conversion and time (see SI), which means that the four recovered supra samples completed the reaction in 24 h despite the differences observed for the first fresh run. This observation confirmed the efficiency of the mechanical interlocking for providing a stable functionalization linkage to the active center responsible of the catalytic activity, in sharp contrast with the labile character of the π interactions established at the supramolecular control examples.

We decided to investigate the scope of the best catalyst (MINT-NPy) by reacting in the same and optimised experimental conditions aromatic aldehydes with different electronic characteristics, such as electron donor (-OH, -OMe) and electron withdrawing groups (-Br, -CHO and -NO_2). The reactivity scope is depicted in Table 2, while kinetic profiles and control examples with (6,5)-SWNT and not-catalysed reactions are shown in the SI.

In general, all the reactions were very clean and the corresponding products were obtained in good to excellent yields within 1–24 h. Interestingly, MINT-NPy sample was able to the Knoevenagel condensation of deactivated aldehydes containing donating groups such as one and two OH moieties (entries 5 and 7), and also a methoxy group (entry 9). In addition, MINT-NPy was able to complete this C-C forming reaction even at room temperature, although 90 h were necessary (entry 10). On the other hand, electron-withdrawing groups showed the expected enhancement in the

Table 1 | Recyclability of MINT catalysts

Catalyst\Cycle[a]	1		2		3		4		5	
	Conv[b]	Time[c]	Conv	Time	Conv	Time	Conv	Time	Conv	Time
MINT-NPy	100	1	99	1	100	1	99	1	98.5	1
MINT-NEt_2	100	3	98.5	3	99.5	3	99	3	100	3

[a]Washing with DCM and new catalytic cycle, [b]Conversion (%) determined by NMR; [c]Time (h).
Recycling studies of catalysts MINT-NPy and MINT-NEt_2.

https://doi.org/10.1038/s42004-025-01591-2

Table 2 | Scope of the MINT-NPy catalyzed Knoevenagel

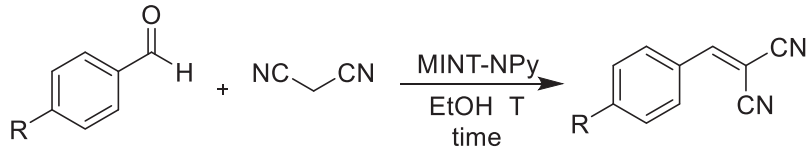

Entry	R	T[b]	Time[c]	Conv[d]	TON[e]	TOF_0[f]
1	H	rt	15.5	100	735	900
2		75	1	100		4140
3	Br	rt	24	97	717	396
4		75	6	97.6	718	1620
5	OH	rt	64	23	169	-
6		75	20	99	734	36
7	OH, OH[g]	rt	64	9	66	-
8		75	33	100	735	-
9	OMe	rt	90	95	698	-
10		75	17	95.5		36
11	CHO[h]	rt	24	90	661	2484
12		75	7	95	698	5400
13	NO_2	rt	1.25	100	735	7380
14		75	0.2	100	735	8820

Scope of the Catalyst MINT-NPy.

[a]Reaction conditions: Substrate (1 mmol), malononitrile (1 mmol), EtOH (3 mL), MINT-NPy (5 mg) for temperature and time.

[b]temperature (°C).

[c]time (h).

[d]conversion, determined by ^{1}H-NMR (%).

[e]turnover number; [f]turnover frequency (h^{-1}), calculated after 5 min of reaction.

[g]Substrate = 3,4-dyhidroxybenzaldehyde.

[h]2 eqs. of malononitrile.

kinetics of the reaction[44]. Terephthaldehyde reacted with 2 equivalents of malononitrile showed higher turnover frequencies than the corresponding model benzaldehyde reaction both at reflux and room temperature conditions (entries 11 and 12). However, time to saturation was larger to accomplish two Knoevenagel reactions in both aldehydes. In addition, nitrobenzaldehyde showed the fastest time of all substrates studied. Reaction at reflux conditions was completed in 12 min with the highest calculated TOF under study, while the product was yielded in 75 min when the reaction was carried out at room temperature. Finally, MINT-NPy was proved to be a very selective catalyst since the condensation of 4-bromobenzaldehyde showed an exquisite selectivity in every situation studied (entries 3 and 4), in sharp contrast with the control samples, in which the selectivity of the reaction fell dramatically (see SI).

Conclusions

We have confirmed that the rational design of MINTs in order to introduce more complex functions can lead to the formation of efficient catalysts. In particular, we use an aniline spacer in the organic macrocycle to graft basic, non-nucleophilic *N*-sites without modifying the structure of the carbon nanotube. Up to 1.6 at. % of N in different chemical groups can be introduced in the surface of the carbon nanotubes making use of the MINT approach.

The basic MINT materials were tested as catalysts in the Knoevenagel condensation. Our samples converted the aldehydes with high activity. Aldehydes with different electronic character can be used. Most remarkably, the linkage of the *N*-basic centers through mechanical bonding allows cyclability, with no loss of activity detected during five cycles of reaction. In comparison, catalysts prepared by direct physisorption of chemically identical macrocycles on the SWNT walls cannot be recycled.

More generally, we demonstrate that MINT building blocks can be used for the modular synthesis of recyclable heterogeneous catalysts that benefit from the inherent high surface area of SWNTs.

Methods

Materials

(6,5)-Enriched single walled nanotubes (6,5-SWNT) were purchased from Sigma-Aldrich (0.7 − 0.9 nm in diameter, length ≥700 nm, mostly semiconducting, 95% purity). Reagents were used as purchased. All solvents were dried according to standard procedures. All air-sensitive reactions were carried out under N_2 atmosphere.

Characterisation methods and synthetic procedures are described in the Supporting Information

MINT sample preparation

The general method for the synthesis of MINTs has been reported elsewhere. Briefly, the nanotubes (10 mg) were suspended in 10 mL of tetrachloroethane through sonication (10 min) and mixed with 0.01 mmol of linear bisalkene U-shaped precursors of the macrocycles mac-NHBoc, and Grubbs' second-generation catalyst at room temperature for 72 h. After this time, the suspension was filtered through a polytetrafluoroethylene (PTFE) membrane of 0.2 µm pore size and the solid washed profusely with dichloromethane (DCM). The solid was resuspended in 10 mL of DCM through sonication for 10 min and filtered through a PTFE membrane of 0.2 µm pore size again. This washing procedure was repeated three times. Sample obtained was denoted as MINT-NHBoc.

Synthesis of MINT-NH_3Cl. MINT-NHBoc was suspended in a 4 M aqueous suspension of HCl with a 4 mg mL^{-1} concentration by 10 min of sonication, and the suspension was magnetically stirred overnight at room temperature. After reaction, the suspension was filtered through polycarbonate (PC) membrane of 0.2 µm pore size, and washed with water till neutral pH was reached. Then, the solid was filtered through a PTFE membrane, washed twice with DCM and finally dried under vacuum. Sample was labeled MINT-NH_3Cl.

Synthesis of MINT-NPy. 5 mg of MINT-NH_3Cl was suspended in 10 ml of ethanol by 10 min of sonication. To this mixture, 0.7 mmol of 2-picolinealdehyde and a drop of formic acid were added. Reaction was maintained under magnetic stirring and reflux conditions for 48 h. After this time, the suspension was filtered through a 0.2 µm pore size PTFE membrane and the solid washed profusely with DCM. The solid was resuspended in 10 mL of DCM through sonication for 10 min and filtered through a PTFE membrane again, and the washing procedure was repeated three times to yield MINT-NPy.

Synthesis of MINT-NEt_2. 5 mg of MINT-NH_3Cl and 0.7 mmol of K_2CO_3 were suspended in 25 ml of ethanol by 10 min of sonication. This mixture was stirred for 5 min, and then 0.7 mmol of ethyliodide was added. Reaction was maintained under magnetic stirring and reflux conditions for 48 h. After this time, the suspension was filtered through a 0.2 µm pore size PTFE membrane and the solid washed profusely with dichloromethane. The solid was resuspended in 10 mL of DCM through sonication for 10 min and filtered through a PTFE membrane again, and the washing procedure was repeated three times to yield MINT-NEt_2.

Synthesis of supramolecular complexes

The synthesis of the supramolecular complexes denoted as SWNT-NHBoc, SWNT-NH_2, SWNT-NPy and SWNT-NEt_2 was performed by the direct mixing of the adequate amounts of (6,5)-SWNT and the corresponding macrocycle to achieve the same functionalisation loading of organic material over the nanotube compared to their respective MINT sample.

Catalysis

The typical catalytic experiment was performed as follows: Aldehyde substrate (1 mmol), malononitrile (1 mmol), solvent (3 mL) and catalyst (5 mg) were mixed in a round bottom flask, stirred magnetically and held at determined temperature (room temperature or 75 °C) for a desired time. At regular intervals, aliquots were withdrawn from the reaction and submitted to NMR spectroscopy analysis to follow the catalytic evolution. Once the reaction was complete, crude mixture concentrated under reduced pressure, yielding the final product. If necessary, attending to the NMR spectra, product was purified by flash chromatography in silica (hexane:ethyl acetate 3:1). In addition, the MINT-containing solid catalysts MINT-NHBoc, MINT-NH_3Cl, MINT-NPy and MINT-NEt_2 were recovered by filtration through a PTFE membrane of 0.2 µm pore-size and washed profusely with DCM. The solid was re-suspended in 10 mL of DCM through sonication for 10 min and filtered through a PTFE membrane of 0.2 µm pore size again. This washing procedure was repeated three times. After drying, the material was submitted to another catalytic run without adding in any case new catalyst precursor.

Data availability

The authors declare that the main data supporting this findings are available within the main text or the Supplementary Information file. All original raw data used to prepare the figures is available at https://repositorio.imdeananociencia.org/home.

Received: 23 October 2024; Accepted: 18 June 2025;
Published online: 16 July 2025

References

1. Liu, D. et al. Chemical Approaches to Carbon-Based Metal-Free Catalysts. *Adv. Mater.* **31**, 1804863 (2019).
2. Bert, M. W. & Yu, J. Recent advances in zeolite chemistry and catalysis. *Chem. Soc. Rev*. **44**, 7022–7025 (2015).
3. Xu, H. & Wu, P. New progress in zeolite synthesis and catalysis. *Natl. Sci. Rev*. **9**, nwac045 (2022).
4. Rajendran, A. et al. Functionalized Silicas for Metal-Free and Metal-Based Catalytic Applications: A Review in Perspective of Green Chemistry. *Chem. Rec.* **20**, 513–540 (2020).

5. Peng, J. et al. Highly efficient and recyclable conversion of CO2 using supported metal-free ionic liquids on ball clay. *Appl. Clay Sci.* **228**, 106645 (2022).
6. Barman, S., Singh, A., Rahimi, F. A. & Maji, T. K. Metal-Free Catalysis: A Redox-Active Donor–Acceptor Conjugated Microporous Polymer for Selective Visible-Light-Driven CO2 Reduction to CH4. *J. Am. Chem. Soc.* **143**, 16284–16292 (2021).
7. Debruyne, M., Van Speybroeck, V., Van Der Voort, P. & Stevens, C. V. Porous organic polymers as metal free heterogeneous organocatalysts. *Green Chem.* **23**, 7361–7434 (2021).
8. Lin, Y. et al. Highly Efficient Metal-Free Nitrogen-Doped Nanocarbons with Unexpected Active Sites for Aerobic Catalytic Reactions. *ACS Nano* **13**, 13995–14004 (2019).
9. Liu, X. & Dai, L. Carbon-based metal-free catalysts. *Nat. Rev. Mater.* **1**, 16064 (2016).
10. Wang, P., Hao, X., Tang, B., Abudula, A. & Guan, G. in *Carbon-Based Metal Free Catalysts* (eds Abdullah Mohammed Ahmed Asiri et al.) 1-19 (Elsevier, 2022).
11. Zhou, J. et al. Tuning the reactivity of carbon surfaces with oxygen-containing functional groups. *Nat. Commun.* **14**, 2293 (2023).
12. Begum, H., Ahmed, M. S. & Kim, Y.-B. Nitrogen-rich graphitic-carbon@graphene as a metal-free electrocatalyst for oxygen reduction reaction. *Sci. Rep.* **10**, 12431 (2020).
13. Melchionna, M., Marchesan, S., Prato, M. & Fornasiero, P. Carbon nanotubes and catalysis: the many facets of a successful marriage. *Cat. Sci Technol.* **5**, 3859–3875 (2015).
14. de Juan, A. et al. Mechanically Interlocked Single-Wall Carbon Nanotubes. *Angew. Chem. Int. Ed.* **53**, 5394–5400 (2014).
15. López-Moreno, A., Villalva, J. & Pérez, E. M. Mechanically interlocked derivatives of carbon nanotubes: synthesis and potential applications. *Chem. Soc. Rev.* **51**, 9433–9444 (2022).
16. Chamorro, R. et al. Reversible dispersion and release of carbon nanotubes via cooperative clamping interactions with hydrogen-bonded nanorings. *Chem. Sci.* **9**, 4176–4184 (2018).
17. Miki, K. et al. Unique Tube–Ring Interactions: Complexation of Single-Walled Carbon Nanotubes with Cycloparaphenyleneacetylenes. *Small* **14**, 1800720 (2018).
18. Balakrishna, B. et al. Dynamic Covalent Formation of Concave Disulfide Macrocycles Mechanically Interlocked with Single-Walled Carbon Nanotubes. *Angew. Chem., Int. Ed.* **59**, 18774–18785 (2020).
19. Cheng, G. et al. Interlocking of Single-Walled Carbon Nanotubes with Metal-Tethered Tetragonal Nanobrackets to Enrich a Few Hundredths of a Nanometer Range in Their Diameters. *ACS Nano* **16**, 12500–12510 (2022).
20. Blanco, M. et al. Positive and negative regulation of carbon nanotube catalysts through encapsulation within macrocycles. *Nat. Commun.* **9**, 2671 (2018).
21. Wielend, D. et al. Mechanically Interlocked Carbon Nanotubes as a Stable Electrocatalytic Platform for Oxygen Reduction. *ACS Appl. Mater. Interfaces* **12**, 32615–32621 (2020).
22. Zhang, W. et al. Mechanical interlocking of SWNTs with N-rich macrocycles for efficient ORR electrocatalysis. *Chem. Sci.* **13**, 9706–9712 (2022).
23. Gianotti, E., Diaz, U., Velty, A. & Corma, A. Strong Organic Bases as Building Blocks of Mesoporous Hybrid Catalysts for C–C Forming Bond Reactions. *Eur. J. Inorg. Chem* **2012**, 5175–5185 (2012).
24. Xue, B., Zhu, J., Liu, N. & Li, Y. Facile functionalization of graphene oxide with ethylenediamine as a solid base catalyst for Knoevenagel condensation reaction. *Catal. Comm.* **64**, 105–109 (2015).
25. Tuci, G. et al. Aziridine-Functionalized Multiwalled Carbon Nanotubes: Robust and Versatile Catalysts for the Oxygen Reduction Reaction and Knoevenagel Condensation. *ACS Appl. Mater. Interfaces* **8**, 30099–30106 (2016).
26. Rana, S., Maddila, S., Pagadala, R. & Jonnalagadda, S. B. Synthesis and characterization of novel bifunctional mesoporous silica catalyst and its scope for one-pot deacetalization–knoevenagel reaction. *J. Porous Mater.* **22**, 353–360 (2015).
27. Qiao, Y., Zhang, L., Li, J., Lin, W. & Wang, Z. Switching on Supramolecular Catalysis via Cavity Mediation and Electrostatic Regulation. *Angew. Chem. Int. Ed.* **55**, 12778–12782 (2016).
28. Onagi, H. & Rebel, J. Jr. Fluorescence resonance energy transfer across a mechanical bond of a rotaxane. *Chem. Commun.* **0**, 4604–4606 (2005).
29. López-Moreno, A. & Pérez, E. M. Pyrene-based mechanically interlocked SWNTs. *Chem. Commun.* **51**, 5421–5424 (2015).
30. Pastorin, G. et al. Double functionalisation of carbon nanotubes for multimodal drug delivery. *Chem. Commun*. 1182–1185 (2006).
31. Fernández-García, L. et al. Graphene anchored palladium complex as efficient and recyclable catalyst in the Heck cross-coupling reaction. *J. Mol. Cat. A* **416**, 140–146 (2016).
32. Shi, R. et al. Palladium/Copper-Catalyzed Oxidative C[BOND]H Alkenylation/N-Dealkylative Carbonylation of Tertiary Anilines. *Angew. Chem. Int. Ed.* **52**, 10582–10585 (2013).
33. Li, H., Yang, Y., Wen, Y. & Liu, L. A mechanism study on preparation of rayon based carbon fibers with (NH4)2SO4/NH4Cl/organosilicon composite catalyst system. *Compos. Sci. Technol.* **67**, 2675–2682 (2007).
34. Sebastian, F. L. et al. Absolute Quantification of sp3 Defects in Semiconducting Single-Wall Carbon Nanotubes by Raman Spectroscopy. *J. Phys. Chem. Lett*. **13**, 3542–3548 (2022).
35. Martínez-Periñán, E. et al. The mechanical bond on carbon nanotubes: diameter-selective functionalization and effects on physical properties. *Nanoscale* **8**, 9254–9264 (2016).
36. Jansen, R. J. J. & Bekkum, H. V. XPS of nitrogen-containing functional groups on activated carbon. *Carbon* **33**, 1021–1026 (1995).
37. Ramanathan, T., Fisher, F. T., Ruoff, R. S. & Brinson, L. C. Amino-Functionalized Carbon Nanotubes for Binding to Polymers and Biological Systems. *Chem. Mater.* **17**, 1290–1295 (2005).
38. Bulusheva, L. G. et al. Electronic state of polyaniline deposited on carbon nanotube or ordered mesoporous carbon templates. *Phys. Status Solidi B* **248**, 2484–2487 (2011).
39. Skowron, S. T. et al. Chemical Reactions of Molecules Promoted and Simultaneously Imaged by the Electron Beam in Transmission Electron Microscopy. *Acc. Chem. Res.* **50**, 1797–1807 (2017).
40. Díaz, U., García, T., Velty, A. & Corma, A. Synthesis and Catalytic Properties of Hybrid Mesoporous Materials Assembled from Polyhedral and Bridged Silsesquioxane Monomers. *Chem. Eur. J.* **18**, 8659–8672 (2012).
41. Sakthivel, B. & Dhakshinamoorthy, A. Chitosan as a reusable solid base catalyst for Knoevenagel condensation reaction. *J. Colloid Interface Sci.* **485**, 75–80 (2017).
42. Pal, S., Khan, N., Karamthulla, S. & Choudhury, L. H. Synthesis of pyranocoumarin fused spirooxindoles via Knoevenagel/Michael/cyclization sequence: a regioselective organocatalyzed multicomponent reaction. *Tetrahedron Lett.* **56**, 359–364 (2015).
43. Gascon, J., Aktay, U., Hernandez-Alonso, M. D., van Klink, G. P. M. & Kapteijn, F. Amino-based metal-organic frameworks as stable, highly active basic catalysts. *J. Catal.* **261**, 75–87 (2009).
44. Forbes, D. C., Law, A. M. & Morrison, D. W. The Knoevenagel reaction: analysis and recycling of the ionic liquid medium. *Tetrahedron Lett.* **47**, 1699–1703 (2006).

Author contributions

M. Vera-Hidalgo and T. Naranjo carried out the synthesis of MINTs, their characterization and the catalytic experiments, M. Blanco designed the modification of MINTs for catalysis, C. Navío carried out the XPS experiment and analysis, L. Ruiz-González, carried out the HRTEM characterization. A. López-Moreno and E. M. Pérez supervised the experimental work and the interpretation of the results, and wrote the manuscript with contributions from all authors.

Competing interests
The authors declare no competing interests.

Additional information
Supplementary information The online version contains supplementary material available at https://doi.org/10.1038/s42004-025-01591-2.

Correspondence and requests for materials should be addressed to Matías Blanco or Emilio M. Pérez.

Peer review information *Communications Chemistry* thanks the anonymous reviewers for their contribution to the peer review of this work. A peer review file is available.